Journal of Applied Physics

RESEARCH ARTICLE | JUNE 02 2022

Ab initio simulations of metal contacts for graphene-based devices

Hancheng Qin ; Wenchang Lu ; J. Bernholc

Journal of Applied Physics 131, 214301 (2022)
https://doi.org/10.1063/5.0091028
CHORUS

AIP Publishing

Journal of Applied Physics ARTICLE scitation.org/journal/jap

Ab initio simulations of metal contacts for graphene-based devices

Cite as: J. Appl. Phys. **131**, 214301 (2022); doi: 10.1063/5.0091028
Submitted: 10 March 2022 · Accepted: 16 May 2022 ·
Published Online: 2 June 2022

Hancheng Qin,[a] Wenchang Lu, and J. Bernholc[a]

AFFILIATIONS

Department of Physics, North Carolina State University, Raleigh, North Carolina 27695-8202, USA

[a]**Authors to whom correspondence should be addressed:** hqin2@ncsu.edu and bernholc@ncsu.edu

ABSTRACT

The precise atomic structure of a metal contact significantly affects the performance of nanoscale electronic devices. We use an accurate, DFT-based non-equilibrium Green's function method to evaluate various metal contacts with graphene or graphene nanoribbons. For surface metal contacts not chemically bound to graphene, Ti contacts have lower resistance than those of Au, Ca, Ir, Pt, and Sr. However, as an edge contact, Ti has larger resistance than Au. Bridging O atoms at Ti and Au edge contacts lowers the transmission by over 30%.

I. INTRODUCTION

The unique electronic structure[1] and exceedingly high intrinsic mobility[2] of graphene make it a propitious material for future high-speed nanoelectronic devices. Fundamental to their functioning are low-resistance metallic contacts. However, the technology to fabricate such contacts easily and reproducibly does not yet exist. Experimental data indicate a wide range of contact resistances[3,4] depending on the metal, the method of fabrication, and contact geometry. Usually, a metal is deposited on the top of a graphene sheet and adheres via van der Waals interactions. This contact geometry is called a surface contact. Much experimental and theoretical work has been performed in this configuration.[5–12] One of the best results was reported for a Pd contact.[13] At a low temperature of 6 K, the resistivity is around 100 $\Omega\mu$m, which is in the ballistic regime. At high temperatures, the resistivity is doubled to ~200 $\Omega\mu$m. However, non-reactive metals result in weak bonding, a long coupling length,[14] and, thus, a large contact resistance. Alternatively, some metals form edge metal–graphene contacts,[15–17] which are chemically bonded. Due to substantial orbital overlaps in such contacts, some experiments found very low contact resistances. Wang *et al.*[18] reported an edge contact in which an encapsulated BN/graphene/BN heterostructure is metalized at both ends and achieved contact resistivity as low as 100 $\Omega\mu$m. The resistance was nearly temperature-independent, in contrast to the Pd surface contact. Robinson *et al.*[19] have shown that a metal–graphene contact resistance dramatically decreases if graphene was pretreated with oxygen plasma.

Since pure graphene is a semimetal and has no bandgap, it cannot be directly used in transistor devices. However, in graphene nanoribbons (GNRs), an energy gap appears[20,21] due to confinement, enabling device applications. Different edge shapes (armchair or zigzag) and ribbon widths modulate the bandgap.[20] For a zigzag edge structure, there should be no bandgap due to band folding from bulk graphene, independent of the nanoribbon width. However, spin polarization at the edge induces a very small bandgap. The armchair edge structures can be categorized into three groups with the number of carbon layers being 3n, 3n + 1, and 3n + 2.[20] The nanoribbons in the 3n + 1 group have the largest bandgap, and those in the 3n + 2 group have the smallest gap. For nanoribbons with mixed edges, the spin polarization effect is reduced, and the bandgap is always small compared to the armchair nanoribbon with a similar width.[22] As the armchair ribbon width increases, the bandgap is reduced because it approaches the zero-gap graphene limit.

Although several theoretical metal–GNR contact studies have been carried out,[23–25] a systematic investigation of tunneling across contacts and the dependence of electron transmission on channel length is lacking. We perform such a study and also compare the performance of surface and edge contacts for best candidate metals.

II. METHODOLOGY

The non-equilibrium Green's function (NEGF) method[26,27] is used to calculate the quantum transport properties, employing the NEGF branch of the real-space multigrid DFT code (RMG).[28–31]

The grid spacing for real-space wave functions and localized orbitals is 0.178 Å, corresponding to 35 Ry kinetic energy cutoff while that for the charge density and potentials is 0.089 Å, corresponding to a 140 Ry plane-wave kinetic energy cutoff. The calculations use norm-conserving pseudopotentials[32] and GGA exchange-correlation functional in the PBE form.[33] The thermally averaged contact resistivities are calculated based on the transmission function Trans(E) as follows:[34]

$$\frac{1}{R_C} = \frac{G_0}{L}\int \mathrm{Trans}(E)\frac{e^{(E-(E_F+eV_G))/k_BT}}{(1+e^{(E-(E_F+eV_G))/k_BT})^2}\frac{dE}{k_BT}, \quad (1)$$

where G_0 is the unit of quantum conductance, L is the width of the contact, V_G is the gate voltage, and the temperature T is set to 300 K.

We consider six metal-surface contacts: Au (111), Ca (111), Ir (111), Pt (111), Sr (111), and Ti (0001). The graphene in the contact region is terminated with hydrogen-saturated zigzag edges, see Fig. 1, for the structure. For surface contacts, Ma *et al.*[8] showed that strongly interacting metals, e.g., Pd, always form chemical bonds to graphene, while weakly interacting metals, like Au, only form bonds through atomic distortions near the edge when the contact length is shorter than 4 Å. Overall, current through metal–graphene surface contacts with contact length longer than 4 Å is not dependent on bonding near the edge.[8] In the following, we investigate the effects of both the channel and contact lengths. For the best surface contact candidate Ti (0001), we also study the resistance of contacts to semiconducting armchair graphene nanoribbons (aGNRs) with different widths. The metals are described by two- or three-layer slabs and are slightly strained in the y-direction so that their lattice constants are commensurate with that of graphene. In all the cases studied here, the lattice-constant changes are smaller than 4%. The optimal equilibrium distances[35] between the metals and the graphene sheet were obtained by minimizing the total energies.

As paradigmatic edge contacts, we examine graphene edge-on attachment to Au and Ti, including oxygen contamination at the contact interface. In each case, the central device structure is optimized until the atomic forces converge to 0.026 eV Å^{-1}. We use the Quantum Espresso code[36] with the PBE exchange-correlation functional[33] to perform structure optimizations. In periodic supercell calculations, 15 Å vacuum regions are added perpendicular to the graphene 2D plane. In NEGF calculations, we found that a very dense k-points mesh is necessary to obtain converged transmission coefficients. We use 251 k-points in the direction perpendicular to the transport axis.

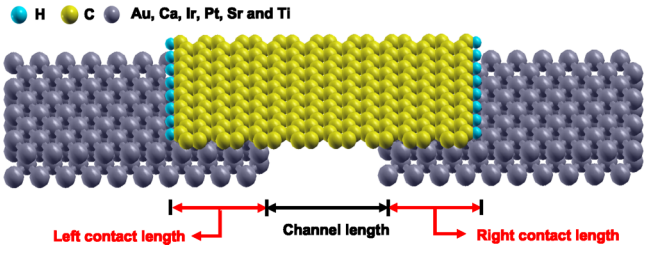

FIG. 1. Atomic structure of the metal–graphene surface contact.

III. RESULTS AND DISCUSSION

A. Metal–graphene surface contacts

For surface metal contacts, the equilibrium distances between the metals and the graphene sheet are listed in Table I. For the Ti–graphene contact, our result of 2.03 Å is very close to 2.05 Å obtained in Ref. 9.

The transmission spectra of all metal–graphene surface contacts considered here are shown in Fig. 2, with the channel length set to 12.8 Å, which is around 3 graphene unit cell lengths. The Ti contact has the best performance at low bias, while the Au contact is the worst. This is also reflected in Table I, which lists calculated zero-bias resistivities. The Ti–graphene surface contact has the lowest resistivity (highest transmission), followed by Ca, Ir, Pt, Sr, and Au.

B. Metal–graphene edge contacts

We study graphene edge contacts to both Au and Ti leads with and without oxygen contamination. The results are presented in Table II. Figure 3 shows a schematic view of Ti–graphene edge contacts. As discussed in Sec. III C, the resistivity of the Ti–G edge contact is much larger than that of the surface contact, independent of the channel length. Kretz *et al.*[16] attribute the increase to the mismatch between the Fermi level states of the metal and those at the graphene edge. With oxygen contamination, the long-channel edge contacts have somewhat larger contact resistance than pristine contacts. This result also agrees with that of Kretz *et al.*

For Au–graphene systems, the edge contact has a much lower resistivity than the surface contact, especially when the channel is long [see Fig. 4(b)]. In the latter case, tunneling between metal leads is suppressed, and the overlap between Au and graphene orbitals at the Fermi level is insufficient for good conductivity because of the large van der Waals bonding distance. In the edge-contact case, chemical bonds at the contact aid in electron transmission. This transmission is only slightly affected by insertion of O atoms into the metal–carbon bonds, which mimics O contamination.

TABLE I. Calculated metal–graphene distances and zero-bias resistivities of metal–graphene surface contacts, with channel length set to 12.8 Å.

Metal	Au	Ca	Ir	Pt	Sr	Ti
Resistivity ($\Omega\mu$m)	158	72	77	90	98	41
Equilibrium distance (Å)—This work	3.41	2.51	3.49	3.53	2.54	2.03
Equilibrium distance (Å)—Other works	3.63	2.24	3.41[35]	3.59	…	2.06

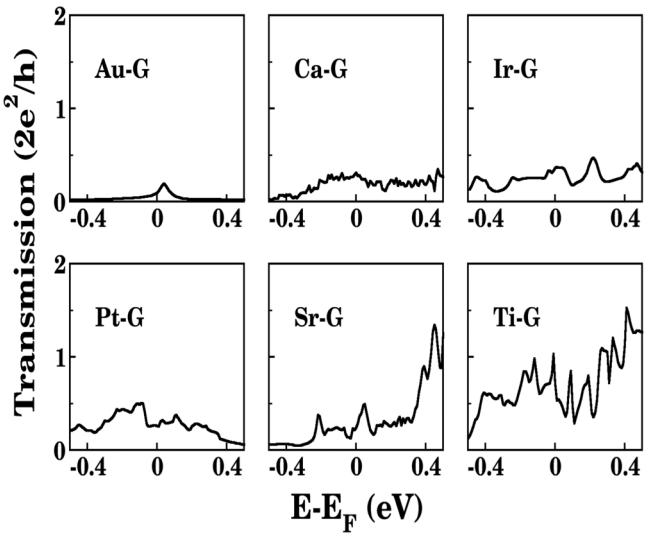

FIG. 2. Transmission spectra of metal–graphene surface contacts considered here.

C. Contact and channel-length effects

For the design of a surface contact, the contact and channel lengths play significant roles. We use Ti to investigate these effects because it performs the best among the six metals considered in Sec. III A. First, we study the effect of contact length, varying the total (left and right) length from 21.3 to 55.4 Å, while the channel length is set to 12.8 Å and fixed. Figure 5(a) shows that different contact lengths lead to very similar I–V curves. These results agree well with those of Ref. 8. We also consider the effect of channel length varying from 12.8 to 166.1 Å, while the contact length is set to 21.3 Å. As Fig. 5(b) demonstrates, the current is high when the channel is short because of tunneling between interface states of

TABLE II. Calculated contact resistivities for different metal–graphene contact types and the longest channel lengths, compared with experimental and theoretical results from the literature.

Contact type	Present results with the longest channel ($\Omega\mu$m)	Experimental results ($\Omega\mu$m)	Prior theoretical results ($\Omega\mu$m)
Ti–G surface contact	273	568[37]	612[9]
Ti–G edge contact	971	…	400[16]
Ti–G edge contact with O	1459	~10 000[18]	600[16]
Au–G surface contact	2382	2000[7]	2284[9]
Au–G edge contact	757	620[38]	320[16]
Au–G edge contact with O	1042	…	…

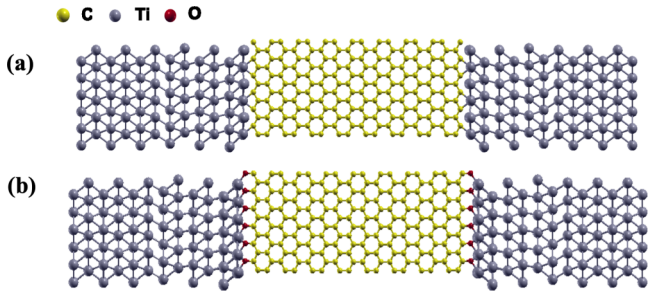

FIG. 3. The schematic view of (a) Ti–graphene edge contact and (b) oxygen-bridged Ti–graphene edge contact.

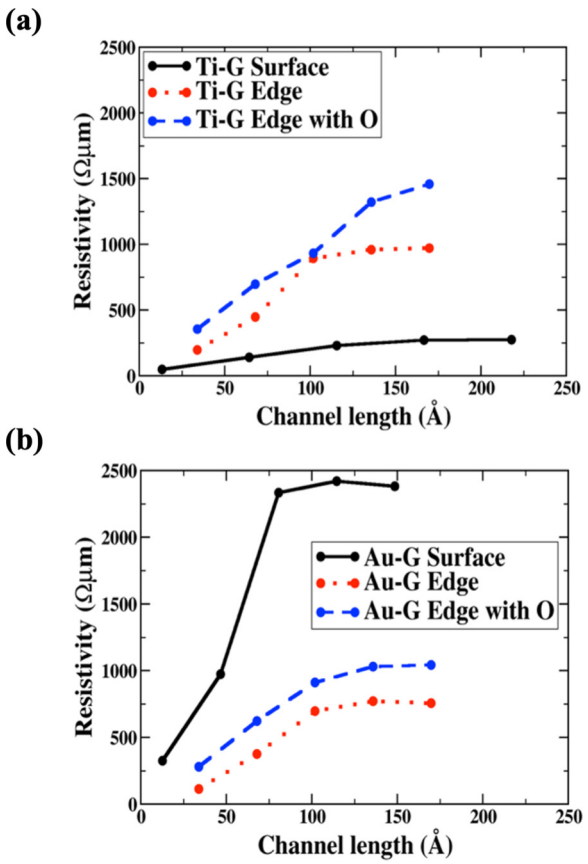

FIG. 4. (a) Zero bias resistivities of Ti–G contacts with different channel lengths. (b) Zero-bias resistivities of Au–G contacts with different channel lengths.

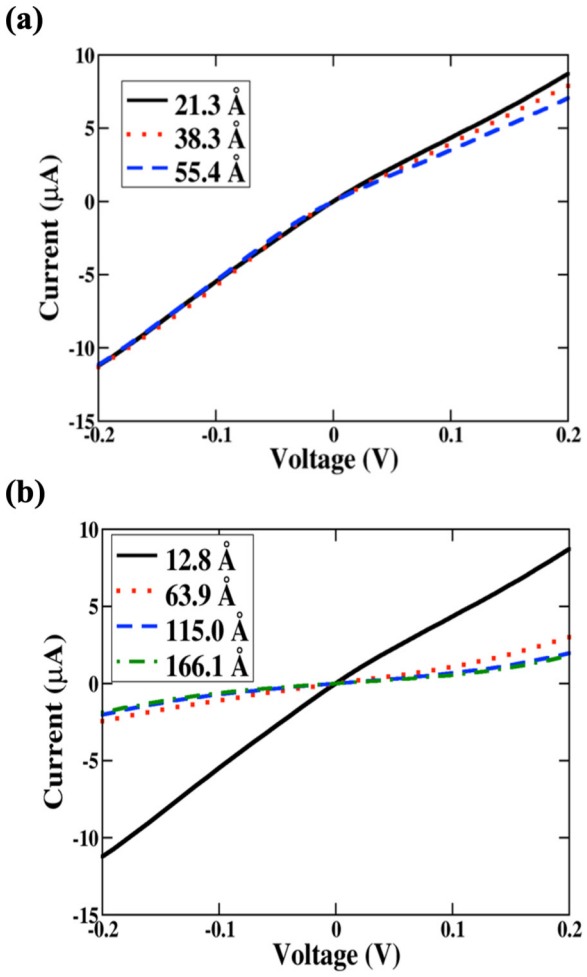

FIG. 5. (a) I–V curves of three Ti–graphene surface contacts with different contact lengths. (b) I–V curves of four Ti–graphene surface contacts with different channel lengths.

the two metal leads. As the channel length increases, interface states' overlap decreases, and its contribution is negligible when the channel length is greater than 115 Å.

Figure 4 shows the channel length effect on the resistivities of Ti or Au contacts. The resistivity is calculated according to Eq. (1)

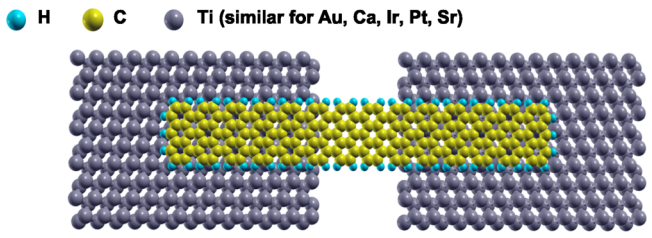

FIG. 6. Atomic structure of a metal–GNR surface contact.

with a bias of 0.1 V. For all of the contacts considered here, the resistivity becomes less dependent on channel length when it exceeds 100 Å, except for the Ti edge contact with O contamination. This is because the calculations are performed in the ballistic regime. For O contamination, hybridization of O orbitals with graphene wave functions plays a more important role in transport properties. Figure 4 also shows that the Ti surface contact has much lower resistivity than its edge contact. For Au contacts, the edge contact performs better than the surface contact.

Table II summarizes our ballistic resistivity results with the longest channel lengths and compares them with prior experimental and theoretical results. One should note that the resistivities in Table II are obtained from the longest channel lengths that we considered, while in Table I the channel length is set to only 12.8 Å and tunneling through overlapping interface states plays an important role in low resistivities listed there. Because ballistic resistivity depends much less on the channel length when it exceeds 100 Å, the resistivities in Table II can be viewed as true metal–graphene contact resistivities for these contact geometries. Our results are in good agreement with the experiment, except for the graphene–Ti edge contact with O contamination, where the experiment shows a much larger resistance. This is likely due to a significantly worse contact geometry in the experiment, potentially due to oxidative damage. Our results are also in quite good agreement with those of prior calculations. The discrepancies are probably due to differences in contact geometries.

D. Metal–aGNR surface contacts

Graphene is a semimetal with a zero-energy gap, which prevents its applications in some electronic devices, such as transistors. A graphene nanoribbon with an armchair edge (aGNR) has a bandgap. aGNRs can be categorized into three families depending on the number of carbon dimer lines n (mod 3) across their widths,[20] 3n, 3n + 1, and 3n + 2. The aGNRs in the 3n + 1 family have the largest bandgaps, and those in the 3n + 2 family have the smallest.[20] Here, we consider 7-, 8-, and 9-aGNRs representing the 3n + 1, 3n + 2, and 3n aGNR families, respectively. Their DFT bandgaps are 1.6, 0.2, and 0.7 eV. Ti is used as the contact metal because it has the lowest resistivity of all the metals tested here. Figure 6 shows the atomic structure of 7-aGNR with a Ti surface contact. Figure 7(a) shows its transmission spectra calculated with different channel lengths.

In the following, we define the transmission gap as an energy window in which the transmission coefficient is smaller than 10^{-3} G_0. Since the 7-aGNR has a bandgap of 1.6 eV, one expects a transmission gap of 1.6 eV if there is no tunneling between the interface states of the metal leads. Figure 7(a) provides clear evidence of tunneling effects when the channel length is short. When the channel length is 12.8 Å, there is no transmission gap and the transmission coefficient is large even at the Fermi level. For longer channel lengths, a transmission gap emerges and increases steadily with the length, eventually reaching the bandgaps of the respective aGNRs,[20] as shown in Fig. 7(b).

It is well known that metal–semiconductor contacts induce metal-induced gap states (MIGS) that decay exponentially as $e^{-x/L}$, where the decay length L is proportional to $1/q$, with q being the

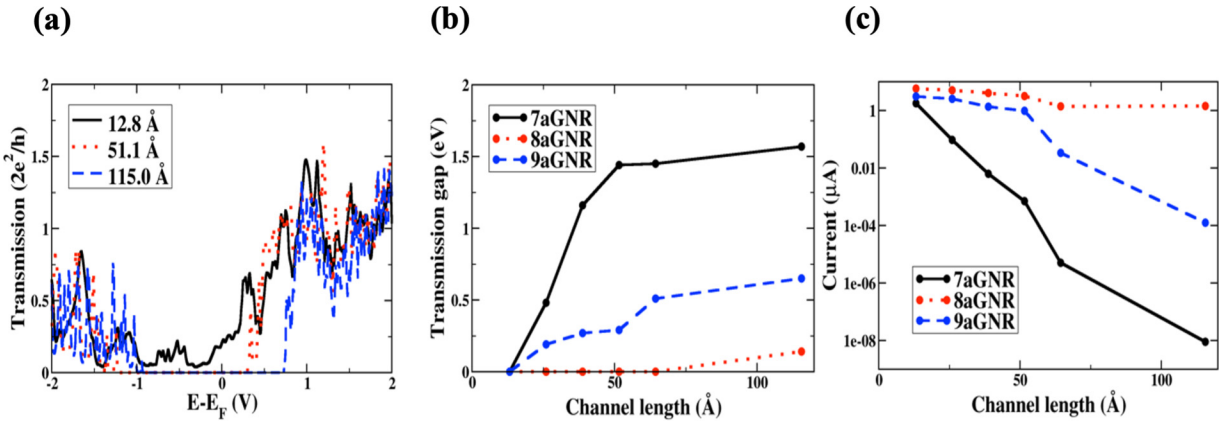

FIG. 7. (a) Transmission spectra of Ti–7aGNR surface contacts with different channel lengths. (b) Transmission gaps of Ti–aGNR surface contacts with different channel lengths. (c) Current across Ti–aGNR surface contacts vs channel length at a bias of 0.1 V.

imaginary part of the wave vector in the gap.[25] This relationship is clearly exhibited in Fig. 7(c), where the currents of all three aGNR contacts decay exponentially. The larger the bandgap, the faster the current decays.

IV. CONCLUSIONS

In summary, we investigated metal–graphene contacts using *ab initio* calculations based on the non-equilibrium Green's function formalism. Different metals with surface- or edge-contact types were explored. We also considered aGNR-based contacts, examining the contact and channel-length effects.

Our results show that among the surface contacts, Ti has the best performance among the considered metals (Ti, Au, Ca, Ir, Pt, and Sr). Contact lengths greater than 10 Å are sufficient. The transmission coefficient converges when the channel length is larger than 115 Å, indicating that overlap and tunneling between interface states of the two contacts vanish at that length. For Ti–aGNR surface contacts with a long channel length, the transmission gap increases and the current decays exponentially with the channel length, confirming this interpretation. Finally, an edge contact is not always a better choice than a surface contact; it depends on the metal choice. Oxygen contamination inhibits transmission at both Ti and Au edge contacts.

ACKNOWLEDGMENTS

This work was supported by US Office of Naval Research under Grant No. N00014-16-1-3153. The supercomputer time was provided by the Oak Ridge Leadership Computing Facility, which is a DOE Office of Science User Facility supported under Contract No. DE-AC05-00OR22725.

AUTHOR DECLARATIONS

Conflict of Interest

The authors have no conflicts to disclose.

DATA AVAILABILITY

The data that support the findings of this study are available from the corresponding authors upon reasonable request.

REFERENCES

[1]P. R. Wallace, "The band theory of graphite," Phys. Rev. **71**, 622 (1947).
[2]K. I. Bolotin, K. J. Sikes, Z. Jiang, M. Klima, G. Fudenberg, J. Hone, P. Kim, and H. L. Stormer, "Ultrahigh electron mobility in suspended graphene," Solid State Commun. **146**, 351 (2008).
[3]F. Giubileo and A. Di Bartolomeo, "The role of contact resistance in graphene field-effect devices," Prog. Surf. Sci. **92**, 143 (2017).
[4]J. M. Marmolejo-Tejada and J. Velasco-Medina, "Review on graphene nanoribbon devices for logic applications," Microelectron. J. **48**, 18 (2016).
[5]Q. Ran, M. Gao, X. Guan, Y. Wang, and Z. Yu, "First-principles investigation on bonding formation and electronic structure of metal-graphene contacts," Appl. Phys. Lett. **94**, 103511 (2009).
[6]S. Russo, M. F. Craciun, M. Yamamoto, A. F. Morpurgo, and S. Tarucha, "Contact resistance in graphene-based devices," Physica E **42**, 677 (2010).
[7]E. Watanabe, A. Conwill, D. Tsuya, and Y. Koide, "Low contact resistance metals for graphene based devices," Diamond Relat. Mater. **24**, 171 (2012).
[8]B. Ma, C. Gong, Y. Wen, R. Chen, K. Cho, and B. Shan, "Modulation of contact resistance between metal and graphene by controlling the graphene edge, contact area, and point defects: An *ab initio* study," J. Appl. Phys. **115**, 183708 (2014).
[9]X. Ji, J. Zhang, Y. Wang, H. Qian, and Z. Yu, "A theoretical model for metal–graphene contact resistance using a DFT–NEGF method," Phys. Chem. Chem. Phys. **15**, 17883 (2013).
[10]M. Ghatge and M. Shrivastava, "Physical insights on the ambiguous metal–graphene interface and proposal for improved contact resistance," IEEE Trans. Electron Devices **62**, 4139 (2015).
[11]Q. Tang, C. X. Zhang, and C. He, "Charge transport properties of graphene: Effects of Cu-based gate electrode," J. Appl. Phys. **7**, 035101 (2016).
[12]T. Cusati, G. Fiori, A. Gahoi, V. Passi, M. C. Lemme, A. Fortunelli, and G. Iannaccone, "Electrical properties of graphene-metal contacts," Sci. Rep. **7**, 1 (2017).
[13]F. Xia, V. Perebeinos, Y. Lin, Y. Wu, and P. Avouris, "The origins and limits of metal–graphene junction resistance," Nat. Nanotechnol. **6**, 179 (2011).
[14]C. Gong, S. McDonnell, X. Qin, A. Azcatl, H. Dong, Y. J. Chabal, K. Cho, and R. M. Wallace, "Realistic metal–graphene contact structures," ACS Nano **8**, 642 (2014).

[15]Y. Matsuda, W.-Q. Deng, and W. A. Goddard, "Contact resistance for 'end-contacted' metal–graphene and metal–nanotube interfaces from quantum mechanics," J. Phys. Chem. C **114**, 17845 (2010).
[16]B. Kretz, C. S. Pedersen, D. Stradi, M. Brandbyge, and A. Garcia-Lekue, "Atomistic insight into the formation of metal-graphene one-dimensional contacts," Phys. Rev. Appl. **10**, 024016 (2018).
[17]V. Passi, A. Gahoi, E. G. Marin, T. Cusati, A. Fortunelli, G. Iannaccone, G. Fiori, and M. C. Lemme, "Ultralow specific contact resistivity in metal–graphene junctions via contact engineering," Adv. Mater. Interfaces **6**, 1801285 (2019).
[18]L. Wang, I. Meric, P. Y. Huang, Q. Gao, Y. Gao, H. Tran, T. Taniguchi, K. Watanabe, L. M. Campos, D. A. Muller, J. Guo, P. Kim, J. Hone, K. L. Shepard, and C. R. Dean, "One-dimensional electrical contact to a two-dimensional material," Science **342**, 614 (2013).
[19]J. A. Robinson, M. LaBella, M. Zhu, M. Hollander, R. Kasarda, Z. Hughes, K. Trumbull, R. Cavalero, and D. Snyder, "Contacting graphene," Appl. Phys. Lett. **98**, 053103 (2011).
[20]Y.-W. Son, M. L. Cohen, and S. G. Louie, "Energy gaps in graphene nanoribbons," Phys. Rev. Lett. **97**, 216803 (2006).
[21]M. Y. Han, B. Özyilmaz, Y. Zhang, and P. Kim, "Energy band-gap engineering of graphene nanoribbons," Phys. Rev. Lett. **98**, 206805 (2007).
[22]J. Jiang, W. Lu, and J. Bernholc, "Edge states and optical transition energies in carbon nanoribbons," Phys. Rev. Lett. **101**, 246803 (2008).
[23]A. Naeemi and J. D. Meindl, "Compact physics-based circuit models for graphene nanoribbon interconnects," IEEE Trans. Electron Devices **56**, 1822 (2009).
[24]H. Liu, H. Kondo, and T. Ohno, "Contact effects of nickel and copper on electron transport through graphene," Phys. Rev. B **86**, 155434 (2012).
[25]C. Archambault and A. Rochefort, "States modulation in graphene nanoribbons through metal contacts," ACS Nano **7**, 5414 (2013).
[26]J. Taylor, H. Guo, and J. Wang, "*Ab initio* modeling of quantum transport properties of molecular electronic devices," Phys. Rev. B **63**, 245407 (2001).
[27]M. Brandbyge, J.-L. Mozos, P. Ordejón, J. Taylor, and K. Stokbro, "Density-functional method for nonequilibrium electron transport," Phys. Rev. B **65**, 165401 (2002).
[28]E. L. Briggs, D. J. Sullivan, and J. Bernholc, "Real-space multigrid-based approach to large-scale electronic structure calculations," Phys. Rev. B **54**, 14362 (1996).
[29]M. B. Nardelli, J.-L. Fattebert, and J. Bernholc, "*O (N)* real-space method for *ab initio* quantum transport calculations: Application to carbon nanotube–metal contacts," Phys. Rev. B **64**, 245423 (2001).
[30]W. Lu, V. Meunier, and J. Bernholc, "Nonequilibrium quantum transport properties of organic molecules on silicon," Phys. Rev. Lett. **95**, 206805 (2005).
[31]See http://www.rmgdft.org for more information about code RMG (accessed 7 March 2022).
[32]D. R. Hamann, "Optimized norm-conserving vanderbilt pseudopotentials," Phys. Rev. B **88**, 085117 (2013).
[33]J. P. Perdew, K. Burke, and M. Ernzerhof, "Generalized gradient approximation made simple," Phys. Rev. Lett. **77**, 3865 (1996).
[34]K. H. Khoo, W. S. Leong, J. T. L. Thong, and S. Y. Quek, "Origin of contact resistance at ferromagnetic metal–graphene interfaces," ACS Nano **10**, 11219 (2016).
[35]C. Busse, P. Lazić, R. Djemour, J. Coraux, T. Gerber, N. Atodiresei, V. Caciuc, R. Brako, A. T. N'Diaye, S. Blügel, J. Zegenhagen, and T. Michely, "Graphene on Ir(111): Physisorption with chemical modulation," Phys. Rev. Lett. **107**, 036101 (2011).
[36]P. Giannozzi, S. Baroni, N. Bonini, M. Calandra, R. Car, C. Cavazzoni, D. Ceresoli, G. L. Chiarotti, M. Cococcioni, I. Dabo, A. Dal Corso, S. de Gironcoli, S. Fabris, G. Fratesi, R. Gebauer, U. Gerstmann, C. Gougoussis, A. Kokalj, M. Lazzeri, L. Martin-Samos, N. Marzari, F. Mauri, R. Mazzarello, S. Paolini, A. Pasquarello, L. Paulatto, C. Sbraccia, S. Scandolo, G. Sclauzero, A. P. Seitsonen, A. Smogunov, P. Umari, and R. M. Wentzcovitch, "QUANTUM ESPRESSO: A modular and open-source software project for quantum simulations of materials," J. Phys.: Condens. Matter **21**, 395502 (2009).
[37]W. Li, C. A. Hacker, G. Cheng, Y. Liang, B. Tian, A. R. Hight Walker, C. A. Richter, D. J. Gundlach, X. Liang, and L. Peng, "Highly reproducible and reliable metal/graphene contact by ultraviolet-ozone treatment," J. Appl. Phys. **115**, 114304 (2014).
[38]V. Passi, A. Gahoi, J. Ruhkopf, S. Kataria, F. Vaurette, E. Pallecchi, H. Happy, and M. C. Lemme, "Contact resistance study of 'edge-contacted' metal-graphene interfaces," in *2016 46th European Solid-State Device Research Conference (ESSDERC)* (IEEE, 2016), pp. 236–239.